High Q-factor microrings using slightly etched rib waveguides

S. Maine(1), D. Marris-Morini(1), L. Vivien(1), E. Cassan(1), D. Pascal(1), S. Laval(1),
B. Han(2), R. Orobtchouk(2), T. Benyattou(2),
L. El Melhaoui(3) and J-M. Fédéli(3)
1) Institut d'Electronique Fondamentale, UMR 8622, Université Paris-Sud, 91405 Orsay, France
2) Laboratoire de Physique de la Matière, UMR 5511, INSA de Lyon, 7, avenue Jean Capelle 69621 Villeurbanne, France
3) Laboratoire d'Electronique de Technologie, de l'Information LETI-Minatec, CEA-G 17 Rue des Martyrs F38054 Grenoble

Abstract: *The paper reports the design, fabrication and characterization of silicon on insulator (SOI) microring resonators using shallow etched rib waveguides. The variation of the Q-factor of the microring resonators as a function of coupling gap between the input waveguide and the ring is studied. Such structures are fabricated using e-beam lithography and reactive ion etching steps. Propagation loss of such rib waveguide has been evaluated lower than 0.8 dB/cm for wavelengths around 1550nm. With a ring diameter of 50µm and a coupling gap of 450nm, the measured Q-factor and finesse are up to 21900 and 28, respectively. The results are matched by numerical optical simulations.*

Introduction

Silicon-on-insulator substrates (SOI) have generated an increasing interest in the recent years, for both microphotonic and microelectronic applications. The thin crystalline silicon film which is separated from the silicon substrate by a buried oxide layer constitutes a high quality optical waveguide at telecommunication wavelengths (from 1.3 µm to 1.6 µm) where silicon is transparent. A very strong light confinement is obtained with SOI structures, due to the large refractive index difference between silicon and its oxide ($\Delta n \approx 2$). This allows the realization of ultra-compact nanophotonic devices and circuits. Among passive structures, waveguides, 90°-turns and beam splitters have been widely studied using either strip or rib waveguides(1).

One of the main optoelectronic devices necessary to realize a high speed optical link is the optical modulator. For few years, several optical modulators integrated in submicron rib SOI waveguides have been proposed (2-4). These structures provide a phase modulation which has to be transformed into an intensity modulation using interferometers such as microring resonators, Fabry-Perot cavity and Mach Zehnder.

We report the design, realisation and characterisation of microring resonators in accord with the constraints established by the proposed modulator devices (5). The characteristics like optical losses, light coupling, and Q-factors are numerically studied and then compared with experimental results for microring resonators on SOI substrates.

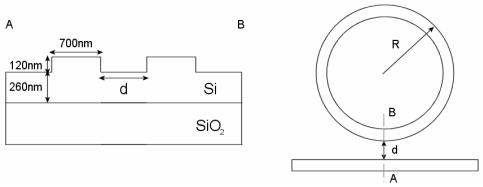

Fig. 1: (a) Cross section schematic view of the designed rib waveguide etched in the silicon layer of SOI. (b) The ring resonator is formed by a ring separated from a waveguide by a distance *d*.

Theory and design

Fig. 1 presents the schematic view of rib waveguide and microring resonator. The waveguide height and width are fixed to 380 nm and 700nm, respectively and the etching depth to 120nm. This rib waveguide ensures single mode propagation for the considered wavelengths: λ=1.3-1.5µm.

A ring resonator is a photonic component composed by a microring waveguide (radius *R*) coupled to an input/output bus waveguide, separated by a distance *d*. The optical transmitted power can be written as:

$$I_t = I_0 \frac{(K+T)^2\tau^2 + T - 2\tau(K+T)|t|\cos(\phi)}{1 + T\tau^2 - 2|t|\tau\cos(\phi)}$$

where I_0 is the incident optical power, *K* the fraction of optical power coupled between the waveguide and the microring, *T* the transmitted optical power coefficient, $|t| = \sqrt{T}$ the field transmission coefficient, P=1-T-K the fraction of lost optical power, $\phi = k_0 n_{eff} L_{eff} = k_0 n_{eff} 2(\pi R)$ the phase shift for a roundtrip along the resonator, $\tau = e^{-\frac{\alpha L_{eff}}{2}} = e^{-\alpha\pi R}$ the attenuation of the field for a roundtrip and α the loss coefficient of the microring. The fraction of optical power coupled in the microring depends on the geometry of the waveguide, which is fixed, on the radius of the microring and on the distance between the microring and the input waveguide *d*.

The quality of the microring resonator is represented by the *Q* factor which depends mainly on two parameters: τ the attenuation of the field and $|t|$ the field transmission coefficient.

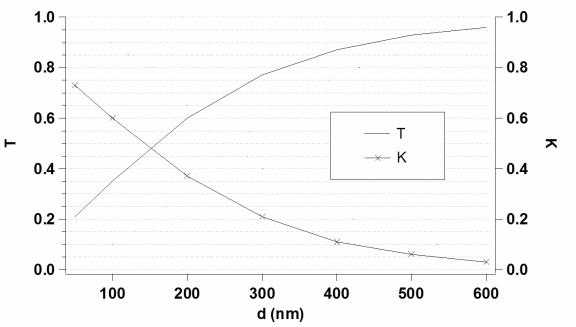

Fig. 2: Fraction of power coupled in the microring (K) and transmitted (T) as a function of the gap d at λ=1.52µm.

Simulation of the coupling between the ring and the waveguide

To numerically study the influence of the gap d (between the waveguide and the microring) on the coupling coefficient, the structure is simulated by a straight waveguide and a portion of a microring resonator with a radius of 50µm. The gap d between the waveguide and the portion of ring is varied from 100nm to 600nm.

The numerical tool was a three-dimensional finite-difference time-domain (FDTD) (6) method with perfectly matched layers as absorbing boundary conditions. The wavelength is fixed to 1.52µm.

From these simulations the fractions of optical power coupled in the microring K and transmitted in the straight waveguide T are determined (Fig. 2). The coupling coefficient K decreases as the gap widens and covers a 3-73% range while T increases from 21% to 96%. Coupling loss, without considering the rib roughness is smaller than 4%.

To validate these simulations, devices with microring resonators were fabricated. The radius of the microrings is fixed to 50µm. To cover a large range of value for the coupling coefficient and taking into account technological constraints, three values of gaps are considered: 200, 300 and 450nm.

Fabrication and measurements

The devices are fabricated on SOI wafers, which have a 400nm thick silicon device layer on a 1µm thick buried silicon oxide (BOX) layer. The thickness of the silicon layer is decreased to 380nm by thermal oxidation. High thermal oxide is deposited to form a hard mask. Electron-beam lithography with negative resist is used. The hard mask is etched down to the silicon layer, followed by a partial etching to 120nm of the silicon to create the rib waveguide. Devices are encapsulated by 500nm of SiO_2 and cleaved into 4.5×9mm dies.

Fig. 3 shows an optical microscope view of the ring resonator device. Input light is split to obtain two balanced branches. The first branch is coupled with a microring and the other one is taken as a reference.

A laser beam from a tuneable laser source with 1530µm centre wavelength is used at TE polarization. Light is coupled to the cleaved facet of the input

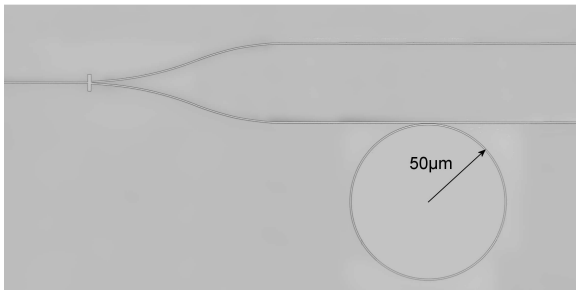

Fig. 3: Optical micrograph of one fabricated microring.

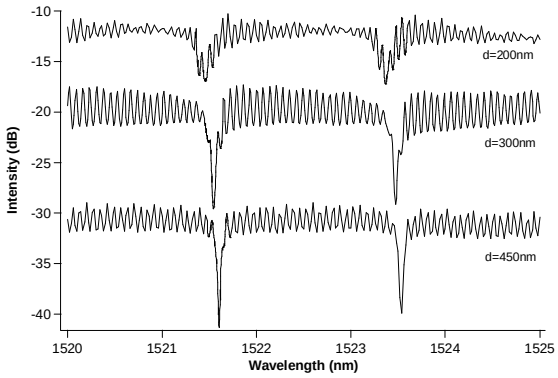

Fig. 4: Measured transmission spectra of microring resonators for gaps of 200, 300 and 450nm and for a radius of 50µm.

waveguide using a lensed fibre. The output beams are collected by a microscope objective and sent on a photodetector. For each device, output power is recorded (Fig. 4) for wavelengths from 1520nm to 1525nm.

The intensity spectrum shows dips which are the consequence of the presence of the microring. The resonant wavelengths and the contrasts depend on the characteristics of the system. Among these: the effective index of the microring, the coupling coefficient and the losses. When the gap varies, the shape of the dip created by the microrings varies as the coupling coefficients change. For a given radius, the losses of the microrings are fixed. So the extinction ratio variation is only due to the gap size variation. The extinction ratio is about 2.5dB for a gap of 200nm and increase to 8dB for d=450nm. So the gap has an important influence on the quality of the resonance.

In addition to the dips created by the microring resonators, small oscillations due to Fabry-Perot resonances between the cleaved ends of the waveguides are clearly observed. In order to dissociate the characteristics of the microrings from Fabry-Perot oscillations, regressions are realized on the measurements. A mathematical function taking into account the parameters of the microring resonator, the Fabry-Perot cavities and the splitter is used. The parameters are the transmission coefficient of the ring t_r, the ring losses τ_r, the group index in the ring n_{gr}, the losses of the straight waveguide τ, the group index of the waveguides n_g, the transmitted fraction of intensity through the cleaved facet T and the losses of the

splitter τ_d. The splitter is supposed to be well balanced.

From theses simulations the values of the parameters are extracted. Concerning the microring itself, the group index n_{gr} is evaluated to 3.79 and the losses to 0.5dB per roundtrip. The interaction between the straight waveguide and the microring is also described. The transmitted intensity coefficient T_r is deduced and is compared to the Finite Difference Time domain (FDTD) simulations (Fig. 5). Measurements are in good agreement with the FDTD calculations previously realized. Both the shape and the values are close to the predicted results.

To evaluate the quality of the microrings independently of the Fabry Perot cavities, the Q-factors are evaluated with the parameters extracted from the measurements. To calculate the Q factor and the finesse of the microrings the following expressions are used:

$$Q = \frac{\lambda_0}{(\Delta\lambda)_{3dB}} = \frac{2\pi n_{gr} L_{eff}}{2\lambda_0 \arccos\left(\frac{2|t_r|\tau_r}{1+|t_r|^2\tau_r^2}\right)}$$

$$\mathcal{F} = \frac{(\Delta\lambda)_{FSR}}{(\Delta\lambda)_{3dB}} = \frac{\pi}{\arccos\left(\frac{2|t_r|\tau_r}{1+|t_r|^2\tau_r^2}\right)}$$

Table 2 gives the values deduced from these expressions. Measured Q-factors as high as 21900 are obtained for a radius of 50µm and a gap of 450nm. For smaller gaps, the Q-factor is lower. This variation can be explained as follow.

For a given radius, the length L_{eff} and the attenuation factor $\tau_r = e^{-\frac{\alpha_r L_{eff}}{2}} = e^{-\alpha_r \pi R}$ are constant.The increase of the Q-factor with the gap is the consequence of the decrease of the coupling coefficient between the microring and the straight waveguide which corresponds to an increase of the transmission coefficient t_r. As the gap is widening, t_r and so the Q-factor, get higher. However to determine an optimum structure, the Q-factor must be considered in parallel with the extinction ratio or contrast of the modulator which tends to zero as t_r tends toward 1.

Conclusions

Microring resonators integrated on SOI substrates using slightly etched rib waveguides have been designed, fabricated by electron beam lithography and characterized. The experimental results on the coupling coefficients between the straight waveguide and the ring are in good agreement with the FDTD simulations. The finesse and quality factor of the microrings have been extracted and Q-factors as high as 21900 have been obtained for 50µm radius microrings and gaps of 450nm.

The small size of microring resonators and high attainable quality factors make them attractive for highly integrated components. Such microrings are especially interesting for the realization of integrated compact modulators.

Table 2: Summary of Q factors and finesses extracted from the measures.

d (nm)	Q-Factor	Finesse
200	8100	10.4
300	13000	16.6
450	21900	28.0

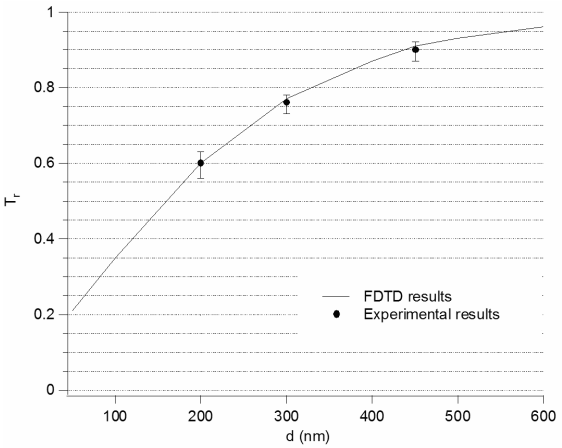

Fig. 5: Comparison between the experimental measurements of the coefficient of transmitted intensity versus the gap for the microring of radii 50µm and 100µm.

Acknowledgments

This work was supported by the French RMNT project "CAURICO" in the frame of collaboration between Institut d'Électronique Fondamentale (CNRS/UPS Orsay), CEA-LETI (Grenoble), Laboratoire de Physique de la Matière (INSA Lyon) and ST-Microelectronics (Crolles). The authors acknowledge the staff of the 200nm cleanroom of the LETI for fabrication of high quality optical structures.

References

1 D. Marris et al, Applied Physics Letters, no 87, 2005.
2 L. Liao et al; Optics Express, no 13, p. 3129, 2005.
3 Q. Xu et al, Nature, no 435, p. 325, 2005.
4 D. Marris et al, J. of Selected Topics in Quant. Elec., no 9, p 747, 2003.
5 S. Maine et al, Proc SPIE 6183, 618360D1-6, 2006.
6 PhotonDesign software, www.photond.com